33rd EPS Conference on Plasma Phys. Rome, 19 - 23 June 2006 ECA Vol.30I, P-2.138 (2006)

Effect of density peaking on Z_{eff} profiles in ASDEX Upgrade H-mode discharges

H. Meister, C. Angioni, B. Kurzan, C. F. Maggi, T. Pütterich, J. Schirmer and ASDEX Upgrade Team

Max-Planck-Institut für Plasmaphysik, EURATOM Assoziation
Boltzmannstr. 2, D-85748 Garching b. München

Introduction The characterisation of the impurity content of a fusion plasma is still an important task as the performance of future burning plasma experiments like ITER will degrade with increasing impurity content. A commonly used quantity characterising the impurity content is the effective charge state $Z_{\mathrm{eff}} = \sum_i n_i Z_i^2 / \sum_i n_i Z_i$ which can be derived e. g. from absolutely calibrated measurements of bremsstrahlung when the radial profiles of electron density n_e and temperature T_e are known. As a weighted average, Z_{eff} will be dominated by the contribution of low Z impurities; impurities such as W give in ASDEX Upgrade a $\Delta Z_{\mathrm{eff}} < 0.3$.

Usually, the measurement of bremsstrahlung is carried out by recording the plasma emission in a certain wavelength range free of line radiation using interference filters and varying types of diodes as detectors. As ASDEX Upgrade continuously increased the amount of its W-coated plasma facing components over the last years, a wider range of impurities might penetrate into the plasma resulting in a broad range of possible line radiation. Therefore it became increasingly important to monitor the spectra used for bremsstrahlung measurements. Thus, a new diagnostic set-up was brought into operation which measures the bremsstrahlung emission spectrally resolved [1]. Furthermore, all available signals measuring bremsstrahlung have been included in one evaluation procedure to deduce one consistent Z_{eff} profile.

Current diagnostic set-up and data evaluation At ASDEX Upgrade bremsstrahlung emission from the plasma is currently measured along the lines-of-sight shown in figure 1, mapped onto a poloidal cross-section. The diagnostic ZEB views the plasma edge at the outer mid-plane in a toroidal cross-section, using 9 toroidally oriented sight-lines. The bremsstrahlung as measured by the charge exchange recombination spectroscopy (CXRS) is included in the deconvolution algorithm, too. The 8 sight-lines of the CXRS are oriented tangentially in the outer mid-plane and cover the whole minor radius. Both diagnostics detect the plasma emission using a Czerny-Turner type spectrograph and a back-illuminated frame-transfer CCD-camera, leading to a good separation of line radiation and

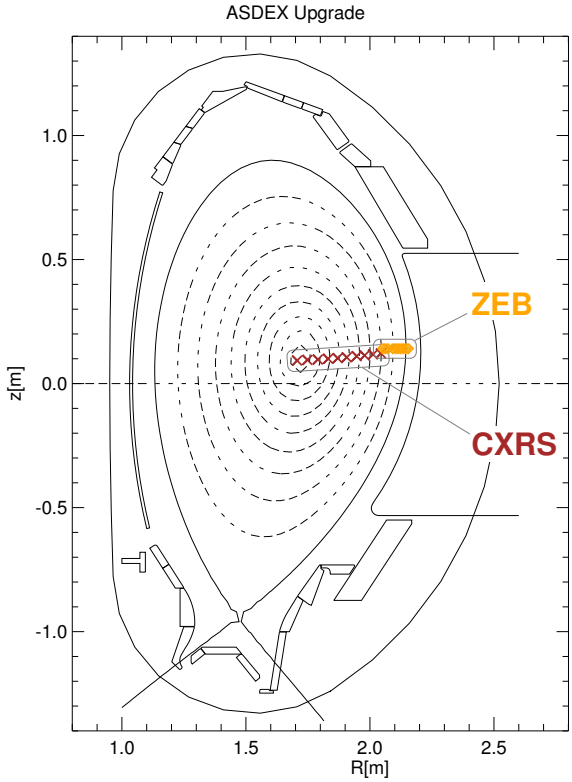

Figure 1: *Sight-lines at ASDEX Upgrade currently measuring bremsstrahlung emission, mapped into a poloidal cross-section.*

bremsstrahlung. For the determination of Z_{eff}, the continuum emission in the measured spectra of both ZEB and CXRS is determined using Bayesian probability theory, giving consistent and improved error statistics. The intensity calibrations of the CXRS and ZEB diagnostic have been refined by using dedicated plasma sweeps accross the sight-lines in order to improve the relative channel-to-channel calibration. The absolute calibration is then fixed in discharges with known low impurity content ($Z_{\mathrm{eff}} \approx 1.5$, see below).

For the deconvolution of Z_{eff} profiles from bremsstrahlung measurements, the profiles of n_e and T_e have to be known. They are usually taken from the evaluation of the Thomson-scattering diagnostic. Further more, calculations of the effective Gaunt-factor have to be performed. At ASDEX Upgrade the formulas given in [2] are used to calculate a tabulated data set, from which the Gaunt-factors can be retrieved very efficiently during data evaluation using spline interpolation. As the Gaunt-factors depend on the charge, the deconvolution of Z_{eff} is iterated until the Gaunt-factors do not change any more. The algorithm adopted for the deconvolution of the bremsstrahlung emissivity, is based on the matrix inversion method and uses curvature minimisation as regularization. A detailed description of its principle and implementation can be found in [3].

Comparison of Z_{eff} with impurity concentrations In order to make a survey over the typical impurities present in H-mode discharges in ASDEX Upgrade, several identical and consecutive discharges were performed. During those discharges, the CXRS diagnostic observed mainly the C and B impurity charge-exchange lines, one per discharge. The B concentration for these discharges is of interest because they were performed directly after a fresh boronization of the vessel. The concentration of He was measured at the plasma edge using charge-exchange-recombination spectroscopy on the Li-beam diagnostic (P2.135, this conference) and dropped rapidly to values about 4% as no He glow-discharges were performed in between shots. Information on the concentration of mid- to high-Z impurities can be obtained from spectroscopic measurements in the wavelength range of $1\,nm - 20\,nm$ (Bragg-Crystal-Spectrometer, Johann-Spectrometer). These evaluate the line emission from He-like O, F and Ne emitting around the separatrix, as well as line emission of W^{46+}, emitting in the plasma centre. Evaluating the Z_{eff} profile for these discharges and comparing it with the contributions of the above mentioned impurities, which add their contribution to Z_{eff} according to $Z_{\mathrm{eff}} = 1 + \sum_i Z_i(Z_i - 1)\frac{n_i}{n_e}$, results in the picture shown in figure 2. In order to compare the local values of He, O, F, Ne and W with the other profiles, a constant distribution over the plasma cross-section has been assumed. As can be seen, within the error bars the impurities add up well to the value of Z_{eff} as measured by bremsstrahlung. The contributions of O, Ne and W are so small in this case, that the plot of their contributions overlaps around the value of zero in figure 2.

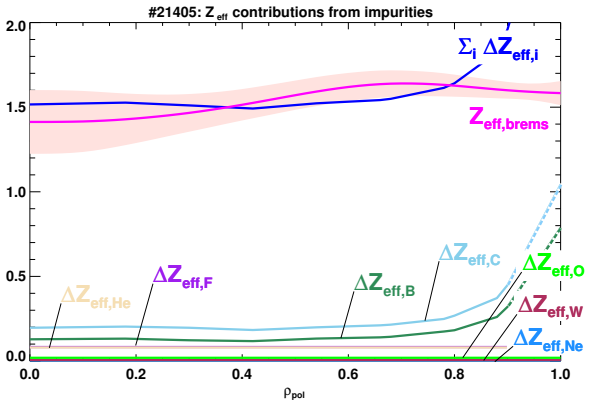

Figure 2: *Comparison of Z_{eff} deduced from bremsstrahlung measurements with individual contributions from several impurities.*

Effect of density peaking on Z_{eff} profiles At ASDEX Upgrade it has been observed that the density profile shape can be controlled via the heating power deposition. As shown in

[4], a power deposition on-axis leads to flat n_e profiles whereas off-axis power deposition results in peaked n_e profile shapes. The present understanding of this behaviour is based on the assumption that the particle transport is coupled to the energy transport ($D \propto \chi$). The off-axis heating leads to very low values of χ in the plasma centre. According to the assumed proportionality, a pinch of the order of the neoclassical Ware pinch is now no longer masked and leads to peaked n_e profiles. With peaked $n_e(\rho)$ a neoclassical pinch should lead to increased impurity influx and thus to peaked $Z_{\mathrm{eff}}(\rho)$. For ICRH heating this was not observed previously despite $n_e(\rho)$ showing the expected peaking (figure 3(a) [5]). In contrast to this, recently performed discharges show exactly the expected behaviour (figure 3(b)).

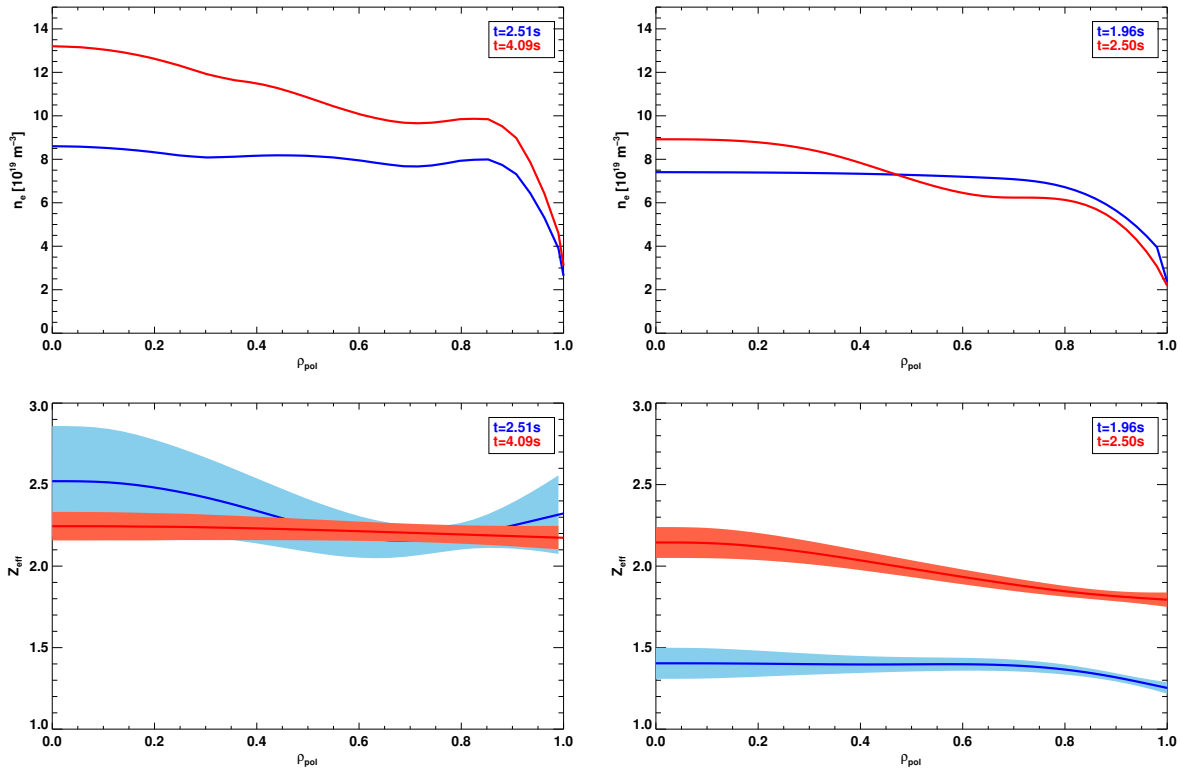

(a) #15122 — old configuration

(b) #21422 — new configuration

Figure 3: *Electron density and Z_{eff} profiles at the beginning and end of a phase with ICRH off-axis heating for old (#15122) and new (#21422) configuration.*

Despite those differences these two discharges seem to be governed by the same neoclassical transport as laid out above. Firstly, ASDEX Upgrade has undergone a significant change during the last two years by replacing more of its plasma facing components with W-coated ones. Right now there are 85% of the surface of the plasma facing components coated with W, including the guard-limiters of the ICRH. In particular, during discharges with ICRH heating an increased influx of impurities has been observed recently (see O2.004/P4.146, this conference). This results in increasing Z_{eff} at the plasma edge for the new configuration (W-coated ICRH limiters, #21422, figure 3(b)) whereas in the old configuration (#15122) Z_{eff} remained constant at the edge (figure 3(a)).

Secondly, there are the differences in the discharges, mainly the different levels of electron density. The discharges, which did not show a peaking in Z_{eff} during off-axis ICRH had

a line-averaged electron density of up to $11.4 \cdot 10^{19} m^{-3}$. This is significantly higher than $6.8 \cdot 10^{19} m^{-3}$ for the one showing the Z_{eff} peaking during ICRH. As diffusion coefficients and drift velocities tend to decrease with increasing n_e (e.g. [6]), high-density discharges are less affected by impurity influx. Thus, one can assume that for the high density case the neoclassical inward pinch of the impurities is too small to show any effect on the Z_{eff} profile, yet. This is supported by the fact, that both discharges lie in the same space of Z_{eff} peaking vs. density peaking (figure 4). Despite the uncertainties being relatively large in this comparison of profile properties, a trend can be seen: for the new configuration values of density peaking were reached, from which on the neoclassical impurity accumulation went beyond recoverable values and the discharge had to be terminated due to radiation peaking from high-Z impurities. For the old configuartion it is to be assumed that a similar scenario would have happened, had the heating not been changed from off-axis ICRH to on-axis NBI. The change in heating scenario was done at a time, at which the onset of impurity accumulation would have been expected from the recent results. Performing a discharge at high density with longer off-axis ICRH heating could clarfiy, if this assumption is valid.

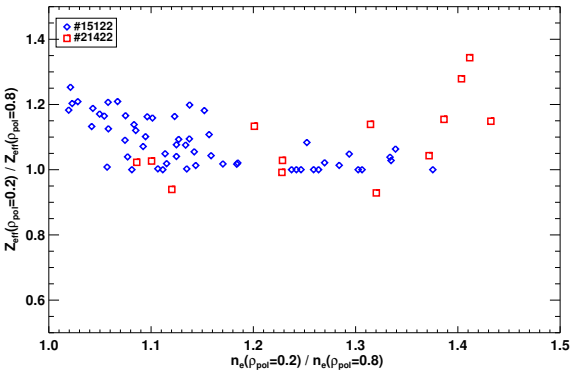

Figure 4: *Z_{eff} peaking vs. density peaking for ICRH off-axis heating in old (#15122) and new (#21422) configuration.*

References

[1] H. Meister *et al.*, Review of Scientific Instruments **75**, 4097 (2004).
[2] W. J. Karzas and R. Latter, Astrophysical Journal — Supplement Series **6**, 167 (1961).
[3] H. Meister *et al.*, Review of Scientific Instruments **74**, 4625 (2003).
[4] J. Stober *et al.*, Nuclear Fusion **41**, 1535 (2001).
[5] H. Meister *et al.*, in *Europhysics Conference Abstracts (CD-ROM, Proc. of the 30th EPS Conference on Controlled Fusion and Plasma Physics, St. Petersburg, 2003)*, edited by R. Koch and S. Lebedev (EPS, Geneva, 2003), Vol. 27A, pp. P–1.136.
[6] F. Wagner and U. Stroth, Plasma Physics and Controlled Fusion **35**, 1321 (1993).